Joint Experimental and Theoretical Characterization of the Electronic Structure of 4,4′-Bis(*N*-m-tolyl-*N*-phenylamino)biphenyl (TPD) and Substituted Derivatives

J. Cornil,*,† N. E. Gruhn,‡ D. A. dos Santos,† M. Malagoli,†,‡ P. A. Lee,‡ S. Barlow,§ S. Thayumanavan,‡,§ S. R. Marder,‡ N. R. Armstrong,‡ and J. L. Brédas†,‡

Laboratory for Chemistry of Novel Materials, Center for Molecular Electronics and Photonics, University of Mons-Hainaut, Place du Parc 20, B-7000 Mons, Belgium, Department of Chemistry, The University of Arizona, 1306 East University Blvd., Tucson, Arizona 85721-0041, and Beckman Institute, California Institute of Technology, Pasadena, California 91125

Received: August 31, 2000; In Final Form: February 23, 2001

We investigate by means of gas-phase ultraviolet photoelectron spectroscopy complemented by quantum-chemical calculations how the frontier levels of the 4,4′-bis(*N*-m-7tolyl-*N*-phenylamino)biphenyl (TPD) molecule are affected upon substitution of the terminal aryl rings with methoxy groups or fluorine atoms. These results provide strategies to modulate energy barriers at metal/organic or organic/organic interfaces involving TPD and its derivatives; it is shown that the change in the energy of the HOMO level of TPD upon derivatization is strongly affected by inductive effects taking place in the σ skeleton.

Introduction

Triarylamine compounds have gained much use as efficient hole transport agents with applications in xerography,[1] organic light-emitting diodes,[2] and electrooptic switches.[3] Recent advances in methodologies for synthesis of triarylamines[4] have made possible the synthesis of a variety of new substituted compounds[4d,5] as well as the incorporation of triarylamine groups into polymers.[6] The ability to synthesize chemically substituted triarylamines allows one to tune the electronic structure of these materials; this is of interest because matching the energy of the highest occupied molecular orbitals of hole transport materials with respect to those of both the anode and electron transport layer strongly influences charge injection efficiencies and the overall performance of organic devices.[5a,7] The design of new materials that could improve both the performance and lifetime of organic-based devices therefore requires a detailed knowledge of the electronic structure of the constituent molecules.

In this study, the electronic structure of a series of triarylamines was investigated by gas-phase photoelectron spectroscopy complemented by semiempirical Hartree−Fock quantum-chemical calculations. The main goal of this study was to provide a better understanding of the impact that substituents on the aryl rings have on the highest occupied molecular orbitals of this class of compounds both in terms of energy and in terms of involvement (inductive vs mesomeric). The compounds studied here are shown in Figure 1; they are all substituted versions of the bis-triarylamine compound 4,4′-bis(*N*-m-tolyl-*N*-phenylamino)biphenyl (TPD), which has commonly been used as the hole transport layer in organic light-emitting diodes. In addition to the determination of the electronic structure of the molecules in the ground state, we have also investigated via configuration-interaction (CI) calculations the characteristics of the intramolecular electron−hole pair (intramolecular exciton) generated in the lowest excited state of these molecules in the isolated state. Our results indicate that the HOMO level and the electron−hole pair in the lowest excited state are primarily confined to the central diamine-biphenyl portion of these molecules. The energy of the HOMO is influenced primarily in an inductive manner by substituents on the external phenyl rings.

Experimental Section

Gas-Phase Photoelectron Spectroscopy. The compounds studied were prepared by the published method.[4d] The He I gas-phase photoelectron spectra were recorded using an instrument that features a 36-cm radius, 8-cm gap hemispherical analyzer and custom designed excitation source, sample cells, detection and control electronics that have been described in more detail previously.[8] The samples were sublimed cleanly with no evidence for decomposition products in the gas phase or as a solid residue. Sublimation temperatures (monitored using a "K" type thermocouple passed through a vacuum feedthrough and attached directly to the sample cell, 10^{-4} Torr) were: TPD, 230−245 °C; TPD-mF, 200−210 °C; TPD-mF2, 230−270 °C; TPD-mF3, 210−280 °C; TPD-pF, 210−220 °C; TPD-mMeO, 220−240 °C; TPD-pMeO, 230−250 °C; NTD (4,4′-bis(*N*-naphthyl-*N*-m-tolylamino)biphenyl; this acronym is used to emphasize that the nitrogen atoms are substituted by naphthyl and tolyl units) 250−270 °C. The argon $^2P_{3/2}$ ionization at 15.759 eV was used as an internal calibration lock of the absolute ionization energy. The difference between the argon $^2P_{3/2}$ ionization and the methyl iodide $^2E_{1/2}$ ionization at 9.538 eV was used to calibrate the ionization energy scale. During data collection, the instrument resolution (measured using the full-width-at-half-height of the argon $^2P_{3/2}$ peak) was 0.020−0.040 eV. All data are intensity corrected with an experimentally determined instrument analyzer sensitivity function. The He I spectra were also corrected for He Iβ resonance line emission from the source, which is about 3% of the intensity of the He Iα line emission and at 1.869 eV higher photon energy.

† University of Mons-Hainaut.
‡ The University of Arizona.
§ California Institute of Technology.

10.1021/jp003142o CCC: $20.00
Published on Web 05/05/2001

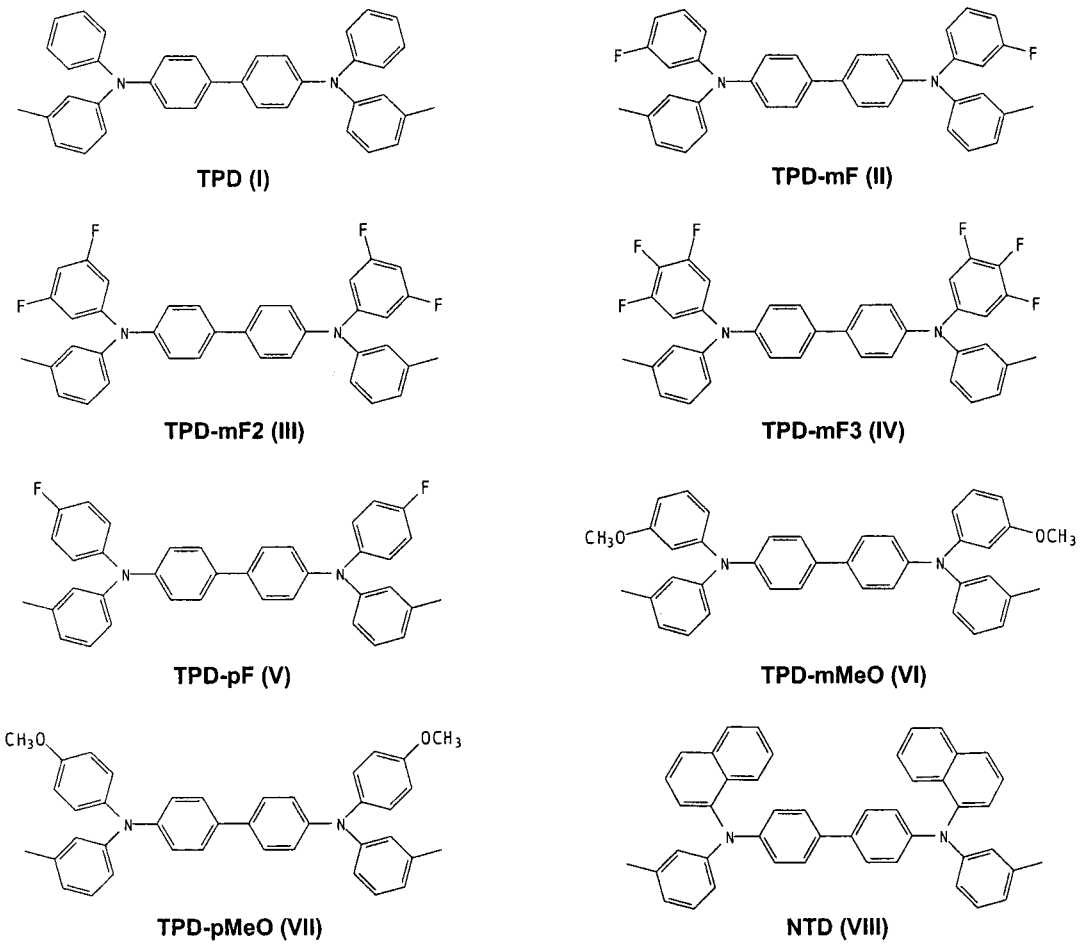

Figure 1. Chemical structures of NTD, TPD, and the substituted derivatives under study.

Theoretical Methodology. Full ground-state geometry optimizations are performed on the compounds using the semiempirical Hartree−Fock Austin Model 1 (AM1) method;[9] this choice is driven by the fact that the AM1 Hamiltonian is parameterized to reproduce the geometric structure and dipole moment of organic molecules in their ground state. The orientation of the methoxy groups in TPD-mMeO and TPD-pMeO is defined in such a way that the oxygen, the methyl carbon and one hydrogen lie in the plane of the ring to which they are attached, as suggested by previous calculations.[10] The charge distributions discussed hereafter are those provided by a Mulliken population analysis at the AM1 level. On the basis of the structural data, we have computed the energy and oscillator strength of the lowest transition of NTD and TPD derivatives by means of the semiempirical intermediate neglect of differential overlap (INDO) Hamiltonian combined to a single configuration interaction scheme (SCI), as developed by Zerner and co-workers;[11] the electronic interaction terms are expressed on the basis of the Mataga−Nishimoto potential. The CI active space involves the configurations generated by the promotion of an electron from one of the highest 10 occupied levels to one of the lowest 10 unoccupied levels. The valence photoelectron spectra have been simulated with the INDO Hamiltonian according to the procedure previously described.[12]

Results and Discussion

Geometries. We first describe some geometric features of the various TPD derivatives and NTD according to the AM1 results. In all cases, the amplitude of the torsion angle between the two phenylene rings of the central biphenyl core is on the order of 38−39°, in agreement with previous gas-phase AM1[13] and ab initio[14] calculations performed on polyparaphenylene oligomers as well as X-ray diffraction experiments on gaseous biphenyl.[15] The two nitrogen atoms have almost pure sp^2 character in TPD and substituted derivatives, which leads to C−N−C bond angles close to 120°; this is consistent with recent AM1, ab initio Hartree−Fock, and density functional theory (DFT) calculations reported on the triphenylamine molecule.[16−18] The three rings connected to each nitrogen atom adopt a propeller-like orientation with torsion angles (plane of the rings with respect to the plane defined by the nitrogen atom and its three attached carbon atoms) varying as a function of the substitution pattern; however, all of the torsion angles are calculated in the range between 30° and 40° while their sum keeps an almost constant value around 103°. Such large torsion angles are in agreement with recent 3-21G ab initio calculations that yield angles of 43.5° in triphenylamine[17] and X-ray crystalline structure analysis of this molecule, giving values from 37.0 to 50.5° among the four inequivalent molecules of the unit cell.[19] It is worth stressing that a large number of almost isoenergetic conformers of the TPD derivatives should coexist in the gas phase; these conformers are related by rotations of ∼180° of the tolyl or substituted phenyl rings around their C−N bond, or by a 180° rotation of the two terminal rings around the bond connecting the nitrogen atoms and the para carbon atoms of the biphenyl core.

In contrast to the geometries calculated at the AM1 level for TPD and the methoxy-substituted and fluorinated TPDs, a weak sp^3 character is obtained for the nitrogen atoms in the NTD molecule; this sp^3 character can be evidenced by a torsion angle

TABLE 1: Energy (in eV) of the HOMO (H) and HOMO-1 (H-1) Levels in NTD, TPD, and Substituted Derivatives, as Inferred from Gas-Phase UPS Spectra and Calculated at the AM1 and INDO Levels[a]

	UPS		AM1			INDO			
molecule	H	H-1	H	H-1	L	H	H-1	L	E_g (OS)
TPD	−6.69	−6.98	−7.73	−8.07	−0.27	−6.74	−7.13	0.21	3.66 (1.14)
TPD-mF	−6.89 *(−0.20)*	−7.18 *(−0.20)*	−7.93 *(−0.20)*	−8.27 *(−0.20)*	−0.44 *(−0.17)*	−6.92 *(−0.18)*	−7.32 *(−0.19)*	0.04 *(−0.17)*	3.67 (1.08)
TPD-mmF2	−7.08 *(−0.39)*	−7.39 *(−0.41)*	−8.12 *(−0.39)*	−8.45 *(−0.38)*	−0.58 *(−0.31)*	−7.08 *(−0.34)*	−7.49 *(−0.36)*	−0.08 *(−0.29)*	3.69 (0.99)
TPD-mmpF3	−7.14 *(−0.45)*	−7.44 *(−0.46)*	−8.23 *(−0.50)*	−8.54 *(−0.47)*	−0.77 *(−0.50)*	−7.24 *(−0.50)*	−7.64 *(−0.51)*	−0.29 *(−0.50)*	3.65 (0.86)
TPD-pF	−6.74 *(−0.05)*	−7.10 *(−0.12)*	−7.86 *(−0.13)*	−8.18 *(−0.11)*	−0.42 *(−0.15)*	−6.89 *(−0.14)*	−7.29 *(−0.16)*	0.04 *(−0.17)*	3.65 (1.09)
TPD-mMeO	−6.75 *(−0.06)*	−7.04 *(−0.06)*	−7.78 *(−0.05)*	−8.11 *(−0.04)*	−0.30 *(−0.03)*	−6.77 *(−0.03)*	−7.17 *(−0.04)*	0.18 *(−0.03)*	3.67 (1.16)
TPD-pMeO	−6.59 *(+0.10)*	−6.95 *(+0.03)*	−7.64 *(+0.07)*	−7.95 *(+0.13)*	−0.24 *(+0.03)*	−6.68 *(+0.06)*	−7.05 *(+0.08)*	0.21 *(0.00)*	3.63 (1.14)
NTD	−6.56 *(+0.13)*	−6.97 *(+0.01)*	−7.71 *(+0.02)*	−8.12 *(−0.05)*	−0.44 *(−0.17)*	−6.75 *(−0.01)*	−7.18 *(−0.05)*	−0.05 *(−0.26)*	3.60 (0.71)

[a] In each case, we report (in parentheses) the energy shifts calculated with respect to the TPD molecule. We also collect for each compound the calculated energy of the LUMO level (L) and the corresponding energy shift with respect to the TPD molecule. The last column provides the lowest transition energy (in eV) and related oscillator strength (OS, in arbitrary units) obtained at the INDO/SCI level.

of 18° between the plane formed by two C−N bonds and the line passing through the third C−N bond. To validate the AM1 geometry, we have used the Gaussian 98 package[20] to perform geometry optimization of the NTD molecule at the DFT B3LYP level, using the gradient-corrected exchange functional by Becke,[21] the correlation functional by Lee, Yang, and Parr,[22] and a 6-31G* basis set. The angle made by the three C−N bonds is calculated to be 10° at the DFT level, thus pointing also to a very weak tendency toward sp^3 character of the nitrogen atoms in the NTD molecule. For the sake of simplicity, we have imposed a pure sp^2 character for the nitrogen atoms to obtain the AM1 and INDO results presented below. The resulting AM1 geometry provides torsion angles for the tolyl and phenylene rings (35° and 29°, respectively) that fall into the typical range obtained for TPD and derivatives; in contrast, a torsion angle of ∼65° is calculated for the naphthyl unit.

Ionization and Orbital Energies. Table 1 collects the energies of the HOMO and HOMO-1 molecular orbitals of NTD, TPD, and its substituted derivatives, as calculated at the AM1 and INDO levels, together with the experimental values from gas-phase UPS spectra; note that slight variations of these values (typically less than 50 meV) are obtained for TPD-mF and TPD-mMeO when going from the conformer sketched in Figure 1 to the one obtained following an ∼180° rotation of the substituted ring around the C−N bond. As reported in a previous study,[12] the gas-phase ionization potential of the TPD molecule calculated at the INDO level (6.74 eV) within the Koopmans' theorem agrees remarkably well with the experimental value (6.69 eV, taken as the vertical ionization energy of the HOMO peak), whereas the AM1 result is overestimated by ∼1.0 eV. The HOMO level of TPD is mostly localized on the biphenyl core, with the largest weights on the para carbon atoms, and on the π-lone pair of the nitrogen atoms; the HOMO-1 level displays very large LCAO coefficients on the nitrogen atoms and much weaker contributions on the four terminal rings.[23,24] The HOMO and HOMO-1 levels have the same energy for all the conformers of TPD obtained upon rotation of the tolyl groups around their C−N bond; in contrast, the conformational effects lead to significant fluctuations in the dipole moment of the molecule, which can be as large as 0.4 D for the TPD molecule at the AM1 level.

The HOMO and HOMO-1 levels of the TPD derivatives are characterized by very small LCAO coefficients on the π-electroactive substituents (i.e., methoxy groups and fluorine atoms); the shifts of the highest two occupied molecular orbitals among the various compounds are therefore mostly driven by inductive effects. This is illustrated in Figure 2 where we have reported the shift of the HOMO energy of the TPD derivatives as a function of the total AM1-calculated charge on the biphenyl core and the nitrogen atoms, which is where the HOMO wave function is primarily localized. The quasi linear correlation between the two quantities demonstrates that the amount of charge transferred to the central part of the TPD backbone is the dominant parameter controlling the energy of the HOMO level. Note that the HOMO energy does not scale linearly with the amount of charge captured by the fluorine atoms; we would then expect the HOMO energy of TPD-mF and TPD-pF to be nearly identical because the net charge on the fluorine atoms is −0.126 |e| in the two derivatives. The AM1- and INDO-calculated shifts of the HOMO energy among the TPD derivatives is in very good agreement with the shifts provided by the gas-phase UPS spectra, see Table 1 and Figure 2; this validates the use of this theoretical approach for the determination of the lowest transition energy of the molecules.

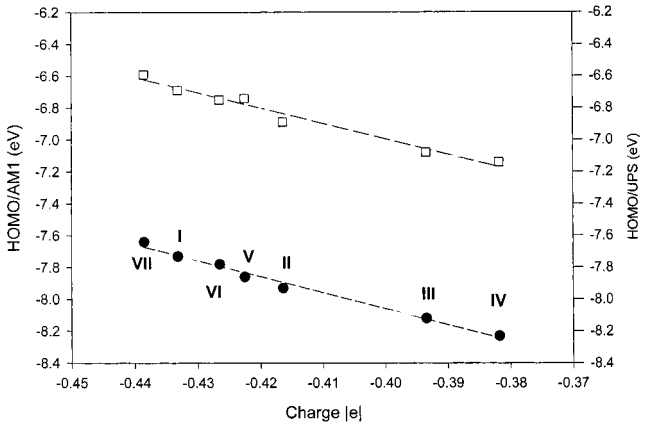

Figure 2. Evolution of the AM1-calculated (filled circles) and experimental (open squares) HOMO energy of TPD and derivatives as a function of the net charge on the biphenyl core and nitrogen atoms; the labels **I→VII** used for the molecules are defined in Figure 1.

The joint experimental and theoretical data thus provide a good basis to estimate the height of energy barriers expected between the highest occupied levels at molecular interfaces in devices based on TPD and derivatives. These values are, however, directly comparable to experimentally determined energy barriers only in situations where: (i) the conformation of the molecules is not significantly affected when going from gas phase to the solid state; (ii) the energies of the frontier levels of the two partners undergo similar shifts induced by solid-state polarization effects; and (iii) the chemical interactions at the interface can be neglected. The origin of such interfacial effects is far from being understood and points to the need for additional theoretical and experimental work.[25]

The shift of the HOMO-1 level of TPD upon derivatization is also mostly governed by inductive effects. However, the

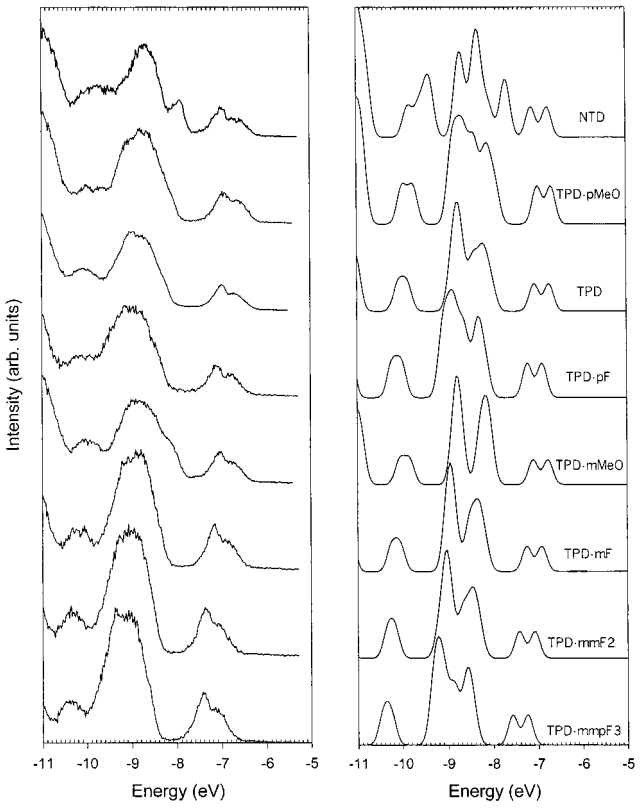

Figure 3. Experimental gas-phase and INDO-calculated UPS spectra of NTD, TPD, and its substituted derivatives. The full-width at half-maximum (fwhm) is set equal to 0.3 eV in the theoretical simulations prior to compression.

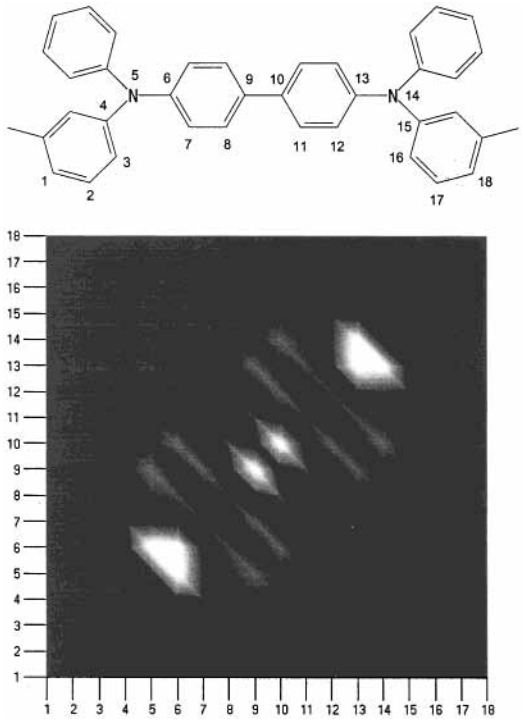

Figure 4. Representation of the electronic wave function of the electron−hole pair photogenerated in the lowest excited state of TPD; each data point (x_i,y_j) on the two-dimensional grid, running along the x and y axes over the carbon atoms labeled in the chemical sketch on top, is associated to the probability $|\psi(x_i,y_j)|^2$ of finding the first particle on site x_i and the second on site y_j. The lightest regions indicate the highest probabilities.

calculated values cannot be related here to a single parameter; they result from a subtle interplay between the LCAO pattern of the molecular orbital and the total charge distribution over the molecule. The INDO energy separations between the HOMO and HOMO-1 levels are systematically overestimated with respect to the experimental values and those calculated at the AM1 level; this is consistent with our recent theoretical works which show that INDO can provide a remarkable description of the low-energy range in the UPS spectra of organic molecules once the binding energy scale has been compressed by a factor of 1.2−1.3;[12,23] the latter is required to compensate somehow for the correlation effects neglected by using Koopmans' approximation.

The electroactive substituents also promote energy shifts of deeper occupied levels. This is shown in Figure 3 where we display the gas-phase UPS spectra of the various molecules together with the corresponding INDO simulations for binding energies down to 11.0 eV. The UPS spectra have been plotted from top to bottom in decreasing order of the experimental HOMO energy. The width of the UPS features has been obtained in the theoretical simulations by using a broadening parameter much smaller than that observed in the experimental curves; we have also normalized the theoretical spectra to the intensity of the most intense peak in the chosen energy range. The UPS spectra of all the TPD derivatives are characterized at low binding energy by a well-separated doublet feature arising from the HOMO and HOMO-1 levels; the different intensities of these two peaks cannot be described by our calculations due to the neglect of photoionization cross sections.[12] The experimental spectra display a broad band at higher ionization energy, typically between 8.0 and 10.0 eV, followed by a less intense peak in the energy range between 10.0 and 11.0 eV; these features are remarkably well reproduced by the INDO simulations which further reveal that the broad unresolved band is actually made of three distinct peaks in most TPD derivatives. Figure 3 also clearly illustrates that the calculated energy shifts of these three bands upon substitution closely match the corresponding experimental evolution. The experimental UPS spectrum of NTD shows the appearance of an additional well-resolved peak on the low-energy side of the broad band resulting from molecular orbitals localized on the naphthyl units, which is well accounted for by the theoretical calculations.[23]

Excited-State Calculations. Despite the significant modulation in the energy of the HOMO level among the TPD derivatives, the energy of the lowest optical transition is weakly affected upon substitution. In all cases, this transition mostly originates from a one-electron excitation between the HOMO and LUMO level; the latter is localized over the central biphenyl core, except for the hexafluorinated derivative (TPD-mmpF3) where significant LCAO coefficients are also found on the substituted phenylene rings. As a result, the electron−hole pair (i.e., exciton) photogenerated in the lowest excited state is confined in the central part of the molecule; it shows a weak extension over the fluorinated phenyl rings only for TPD-mmpF3.

The localization of the exciton is illustrated in Figure 4 in the case of TPD via a wave function analysis carried out at the INDO/SCI level. The plot in Figure 4 is a two-dimensional grid running along each axis over all of the atoms labeled in the chemical sketch on top of the Figure; each data point (x_i,y_j) corresponds to the probability $|\psi(x_i,y_j)|^2$ of finding the electron on site x_i and the hole on site y_j (or vice versa). The probability amplitude ψ(p,q) to have a particle in orbital p on site x_i (i.e., s, p_x, p_y or p_z orbital) and the other particle in orbital q on site

y_j is given by

$$\psi(\mathrm{p,q}) = 1/\sqrt{2}[\sum_r C_r^{\mathrm{CI}}\, C_{\mathrm{p}}^{\mathrm{LCAO}}\,(\mathrm{e}^-) C_{\mathrm{q}}^{\mathrm{LCAO}}\,(\mathrm{h}^+) + \sum_j C_r^{\mathrm{CI}}\, C_{\mathrm{p}}^{\mathrm{LCAO}}(h^+) C_{\mathrm{q}}^{\mathrm{LCAO}}\,(\mathrm{e}^-)] \quad (1)$$

where $C_{\mathrm{p}}(\mathrm{h}^+)$ and $C_{\mathrm{p}}(\mathrm{e}^-)$ are the LCAO (linear combination of atomic orbitals) coefficients in the occupied and unoccupied levels, respectively, that are involved in the *r*th singly excited configuration (with C_r^{CI} being the associated CI coefficient). The lightest (darkest) zones of the graph correspond to the highest (lowest) probabilities of finding the particles at the positions defined by the grid. The orthonormalization of the basis set requires that

$$\sum_{\mathrm{p}} \sum_{\mathrm{q}} |\psi(\mathrm{p,q})|^2 = 1 \quad (2)$$

The energy shifts of the LUMO level calculated for the series of TPD derivatives parallel those obtained for the HOMO level (see Table 1); this rigid shift points to the major role played by inductive effects in the σ skeleton in determining the position of the frontier levels and rationalizes the absence of significant shifts in the lowest optical transition energies upon substitution. These results contrast with those of previous INDO calculations performed on oligo(phenylenevinylene)s substituted by cyano and/or methoxy groups; there, π-mesomeric effects induce a high asymmetry in the shifts of the HOMO and LUMO levels,[26] which in turn leads to significant shifts of the lowest optical transition as a function of the nature, number, and position of the electroactive substituents attached to the conjugated backbone.[26]

The nature of the lowest excited state markedly differs for NTD because the LUMO and LUMO+1 levels are centered on the naphthyl units and the LUMO+2 on the biphenyl core. The lowest optical transition of this compound is mainly described by the mixing of three one-electron excitations: 52.2%, 24.5%, and 10% from the H→L, H-1→L+1, and H→L+2 excitations, respectively. This leads to a photogenerated electron−hole pair delocalized over the central part of the molecule and the naphthyl units of NTD, as illustrated in Figure 5. The pronounced charge-transfer character of the two dominant configurations can be used to rationalize the significant drop in oscillator strength when going from TPD to NTD; the intensity is actually redistributed among several optical transitions at higher energy, whose description is beyond the scope of the present paper.

Conclusions

Gas-phase UPS spectra and corresponding quantum-chemical calculations demonstrate that the energy of the HOMO level of the 4,4′-bis(*N*-m-tolyl-*N*-phenylamino)biphenyl (TPD) molecule can be modulated upon substitution of the terminal rings by methoxy groups and fluorine atoms in various numbers and/or positions. The energy shifts are mostly governed by inductive effects taking place within the σ skeleton. The present results thus demonstrate that energy barriers in electrooptic devices can be fine-tuned through molecular engineering of a given conjugated backbone.

The various substitution patterns lead to very similar shifts of the HOMO and LUMO levels. As a result, the energy of the lowest optical transition of the TPD molecule, that is mainly described by an excitation between these two frontier electronic levels, is only weakly affected by derivatization of the external rings.

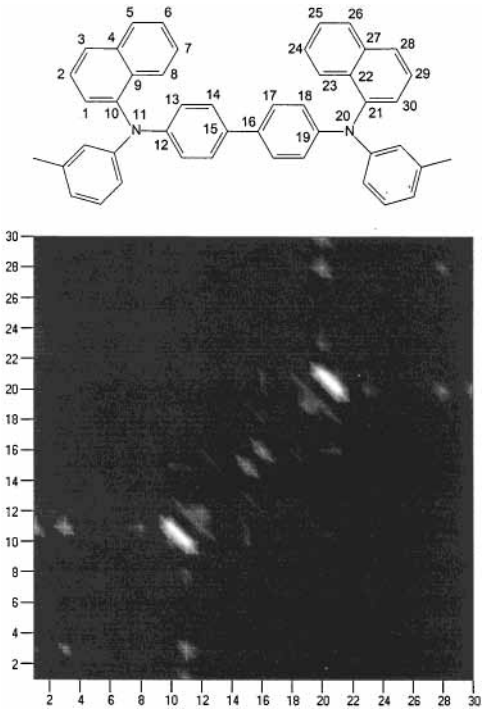

Figure 5. Representation of the electronic wave function of the electron−hole pair photogenerated in the lowest excited state of NTD; each data point (x_i,y_j) on the two-dimensional grid, running along the *x* and *y* axes over the carbon atoms labeled in the chemical sketch on top, is associated to the probability $|\psi(x_i,y_j)|^2$ of finding the first particle on site x_i and the second on site y_j. The lightest regions indicate the highest probabilities.

Acknowledgment. This work has been partly supported by the Belgian Federal Government (Pôle d'Attraction Interuniversitaire en Chimie Supramoléculaire et Catalyse, PAI 4/11); the Belgian National Fund for Scientific Research (FNRS); Office of Naval Research (ONR) through the MURI Center for Advanced Multifunctional Nonlinear Optical Polymers and Molecular Assemblies (CAMP) and the National Science Foundation (CHE-0078819); and the Francqui Foundation, Belgium, through award of a postdoctoral fellowship to M.M. The measurements of the gas-phase UPS spectra were carried out in the Center for Gas-Phase Electron Spectroscopy, The University of Arizona. J.C. is Research Associate of the FNRS.

References and Notes

(1) (a) Borsenberger, P. M.; O'Regan, M. B. *Chem. Phys.* **1995**, *200*, 257. (b) Borsenberger, P. M.; Bruenbaum, W. T.; Magin, E. H. *Physica B* **1996**, *228*, 226. (c) Visser, S. A.; Gruenbaum, W. T.; Magin, E. H.; Borsenberger, P. M. *Chem. Phys.* **1999**, *240*, 197.

(2) (a) Tang, C. W.; Van Slyke, S. A. *Appl. Phys. Lett.* **1987**, *51*, 913. (b) Mori, T.; Obata, K.; Imaizumi, K.; Mizutani, T. *Appl. Phys. Lett.* **1996**, *69*, 3309. (c) Jordan, R. H.; Rothberg, L. J.; Dodabalapur, A.; Slusher, R. E. *Appl. Phys. Lett.* **1996**, *69*, 1997. (d) Kalinowski, J.; Di Marco, P.; Cocchi, M.; Fattori, V.; Camaioni, N. *Appl. Phys. Lett.* **1996**, *68*, 2317. (e) Dodabalapur, A. *Solid State Commun.* **1997**, *102*, 259. (f) Yamamori, A.; Adachi, C.; Koyama, T.; Taniguchi, Y. *J. Appl. Phys.* **1999**, *86*, 4369.

(3) Miller, R. D.; Lee, V. Y.; Twieg, R. J. *Chem. Commun.* **1995**, 245 and references therein.

(4) (a) Beller, M. *Angew. Chem., Int. Ed. Engl.* **1995**, *34*, 1316. (b) Driver, M. S.; Hartwig, J. F. *J. Am. Chem. Soc.* **1996**, *118*, 7217. (c) Wolfe, J. P.; Wagaw, S.; Buchwald, S. L. *J. Am. Chem. Soc.* **1996**, *118*, 7215. (d) Thayumanavan, S.; Barlow, S.; Marder, S. R. *Chem. Mater.* **1997**, *9*, 3231. (e) Marcoux, J.-F.; Wagaw, S.; Buchwald, S. L. *J. Org. Chem.* **1997**, *62*, 1568. (f) Goodbrand, H. B.; Hu, N.-X. *J. Org. Chem.* **1999**, *64*, 670.

(5) (a) Koene, B. E.; Loy, D. E.; Thompson, M. E. *Chem. Mater.* **1998**, *10*, 2235. (b) O'Brien, D. F.; Burrows, P. E.; Forrest, S. R.; Koene, B. E.; Loy, D. E.; Thompson, M. E. *Adv. Mater.* **1998**, *10*, 1108. (c) Thelakkat, M.; Schmitz, C.; Hohle, C.; Strohriegl, P.; Schmidt, H.-W.; Hofmann, U.; Schloter, S.; Haarer, D. *Phys. Chem. Chem. Phys.* **1999**, *1*, 1693. (d) Uekawa, M.; Miyamomo, Y.; Ikeda, H.; Kaifu, K.; Ichi, T.; Nakaya, T. *Thin Solid Films* **1999**, *352*, 185. (e) Watanabe, M.; Yamamoto, T.; Nishiyama, M. *Chem. Commun.* **2000**, 133.

(6) (a) Bellmann, E.; Shaheen, S. E.; Thayumanavan, S.; Barlow, S.; Grubbs, R. H.; Marder, S. R.; Kippelen, B.; Peyghambarian, N. *Chem. Mater.* **1998**, *10*, 1668. (b) Li, X.-C.; Liu, Y.; Liu, M. S.; Jan, A. K.-Y. *Chem. Mater.* **1999**, *11*, 1568. (c) Bellmann, E.; Shaheen, S. E.; Grubbs, R. H.; Marder, S. R.; Kippelen, B.; Peyghambarian, N. *Chem. Mater.* **1999**, *11*, 399. (d) Shaheen, S. E.; Jabbour, G. E.; Kippelen, B.; Peyghambarian, N.; Anderson, J. D.; Marder, S. R.; Armstrong, N. R.; Ballmann, E.; Grubbs, R. H. *Appl. Phys. Lett.* **1999**, *74*, 3212.

(7) (a) Van Slyke, S. A.; Chen, C. H.; Tang, C. W. *Appl. Phys. Lett.* **1996**, *69*, 2160. (b) Jonda, C.; Mayer, A. B. R.; Thalekkat, M.; Schmidt, H.-W.; Schreiber, A.; Haarer, D.; Terrell, D. *Adv. Mater. Opt. Electron.* **1999**, *9*, 117. (c) Hill, I. G.; Kahn, A. *J. Appl. Phys.* **1999**, *86*, 2116. (d) Biebeler, C.; Antoniudis, H.; Bradley, D. D. C.; Shirota, Y. *J. Appl. Phys.* **1999**, *85*, 608. (e) Yamashita, K.; Mori, T.; Mizutani, T.; Miyazaki, H.; Takeda, T. *Thin Solid Films* **2000**, *363*, 33.

(8) Westcott, B. L.; Gruhn, N. E.; Enemark, J. H. *J. Am. Chem. Soc.* **1998**, *120*, 3382 and references therein.

(9) Dewar, M. J. S.; Zoebisch, E. G.; Healy, E. F.; Stewart, J. J. P. *J. Am. Chem. Soc.* **1995**, *107*, 3902.

(10) Lhost, O.; Brédas, J. L. *J. Chem. Phys.* **1992**, *96*, 5279.

(11) Zerner, M. C.; Loew, G. H.; Kichner, R. F.; Mueller-Westerhoff, U. T. *J. Am. Chem. Soc.* **1980**, *102*, 589.

(12) Cornil, J.; Vanderdonckt, S.; Lazzaroni, R.; dos Santos, D. A.; Thys, G.; Geise, H. J.; Yu, L. M.; Szablewski, M.; Bloor, D.; Logdlund, M.; Salaneck, W. R.; Gruhn, N. E.; Lichtenberger, D. L.; Lee, P. A.; Armstrong, N. R.; Brédas, J. L. *Chem. Mater.* **1999**, *11*, 2436.

(13) Zojer, E.; Cornil, J.; Leising, G.; Brédas, J. L. *Phys. Rev. B* **1999**, *59*, 7957.

(14) (a) Brédas, J. L.; Themans, B.; Fripiat, J. G.; André, J. M.; Chance, R. R. *Phys. Rev. B* **1984**, 29, 6761. (b) Brédas, J. L.; Street, G. B.; Themans, B.; Andre, J. M. *J. Chem. Phys.* **1985**, *83*, 1323.

(15) Bastiansen, O. *Acta Chem. Scand.* **1949**, *3*, 408.

(16) Sakanoue, K.; Motoda, M.; Sugimoto, M.; Sakaki, S. *J. Phys. Chem.* **1999**, *103*, 5551.

(17) Pacansky, J.; Waltman, R. J.; Seki, H. *Bull. Chem. Soc. Jpn.* **1997**, *70*, 55.

(18) Malagoli, M.; Brédas, J. L. *Chem. Phys. Lett.* **2000**, *327*, 13.

(19) Sobolev, A. N.; Belsky, V. K.; Romm, I. P.; Chernikova, N. Y.; Guryanova, E. N. *Acta Crystallogr. C* **1985**, 41, *967.*

(20) Gaussian 98, Revision A.7; Frisch, M. J.; Trucks, G. W.; Schlegel, H. B.; Scuseria, G. E.; Robb, M. A.; Cheeseman, J. R.; Zakrzewski, V. G.; Montgomery, J. A., Jr.; Stratmann, R. E.; Burant, J. C.; Dapprich, S.; Millam, J. R.; Daniels, A. D.; Kudin, K. N.; Strain, M. C.; Farkas, O.; Tomasi, J.; Barone, V.; Cossi, M.; Cammi, R.; Mennucci, B.; Pomelli, C.; Adamo, C.; Clifford, S.; Ochterski, J.; Petersson, G. A.; Ayala, P. Y.; Cui, Q.; Morokuma, K.; Malick, D. K.; Rabuck, A. D.; Raghavachari, K.; Foresman, J. B.; Cioslowski, J.; Ortiz, J. V.; Baboul, A. G.; Stefanov, B. G.; Liu, G.; Liashenko, A.; Piskorz, P.; Komaromi, I.; Gomperts, R.; Martin, R. L.; Fox, D. J.; Keith, T.; Al-Laham, M. A.; Peng, C. Y.; Nanayakkara, A.; Gonzalez, C.; Challacombe, M.; Gill, P. M. W.; Johnson, B.; Chen, W.; Wong, M. W.; Andres, J. L.; Gonzalez, C.; Head-Gordon, M.; Replogle, E. S.; Pople, J. A. Gaussian, Inc.: Pittsburgh, PA, 1998.

(21) Becke, A. D. *Phys. Rev. A* **1988**, *38*, 3098.

(22) Lee, C.; Yang, W.; Parr, R. G. *Phys. Rev. B* **1988**, *38*, 785.

(23) Hill, I. G.; Kahn, A.; Cornil, J.; dos Santos, D. A.; Brédas, J. L. *Chem. Phys. Lett.* **2000**, *317*, 444.

(24) Sugiyama, K.; Yoshimura, D.; Miyamae, T.; Miyazaki, T.; Ishii, H.; Ouchi, Y.; Seki, K. *J. Appl. Phys.* **1998**, *83*, 4928.

(25) Ishii, H.; Sugiyama, K.; Ito, E.; Seki, K. *Adv. Mater.* **1999**, *11*, 605.

(26) Cornil, J.; dos Santos, D. A.; Beljonne, D.; Brédas, J. L. *J. Phys. Chem.* **1995**, *99*, 5604.